



Trade Science Inc.

Materials Science

An Indian Journal

Full Paper

MSAIJ, 3(4), 2007 [225-229]

Fabrication, morphology and structural characterization of tungsten oxide nanorods

T.Maiyalagan, B.Viswanathan*

National Center for Catalysis Research, Department of Chemistry, Indian Institute of Technology Madras, Chennai 600 036, (INDIA)

Phone : +91-044-22574200 ; Fax: +91-44-22574202

E-mail : bvnathan@iitm.ac.in

Received: 1st September, 2007 ; Accepted: 6th September, 2007

ABSTRACT

The Template synthesis of Tungsten oxide nanorods by calcination of Phosphotungstic acid (HPW) on alumina membrane template is described. The nanorods were characterized by electron microscopic analyses, Raman, IR and X-ray diffraction techniques. SEM, TEM and AFM images reveal the hollow structures and vertically aligned features of the nanotubes and the phase structure of the WO_3 was proved by X-ray diffraction. In addition, it is observed that the cycle ability of the nanorods is superior to that of bulk materials, which implies that the morphology has an influence on the electrochemical performances of the material.

© 2007 Trade Science Inc. - INDIA

KEYWORDS

Tungsten oxide nanorods;
Template synthesis;
Alumina template.

INTRODUCTION

There is great interest in the synthesis of one-dimensional nanostructured materials because of its potential applications in many areas. Metal-oxide semiconductors such as WO_3 , TiO_2 , and ZnO and SnO_2 are widely used in sensors, having high detection ability and stability^[1-3]. These transition metal oxides have drawn much attention from scientists in recent years because they are applied as electrochromic materials. Their potential applications include several technological areas. Tungsten metal, tungsten oxides and tungstates represent a fascinating class of materials. Tungsten wires/filaments are widely used as tips for field emission and tips for scanning tunneling microscopy^[4].

The rich structural chemistry of tungsten oxides encompasses a multitude of interesting compounds and a wide spectrum of tungstic acids and different WO_3 phases. Tungsten oxide is an important functional material. In recent years, a variety of nanometer-scaled structures of tungsten oxide have been developed. These nano structures have demonstrated promising properties. To date, WO_3 has been one of the most extensively studied materials for its Electrochromic, photochromic and thermo chromic properties for use in devices, such as information displays, sensor devices and smart Windows. In addition, WO_3 has a high potential for use in electrochemical devices, such as rechargeable lithium batteries, owing to its rich chemical intercalation reactivity. The oxides of transition metal tungsten have at-

Full Paper

tracted constant research interest for the past few decades due to their wide applicability as gas sensors for SO_2 and H_2S ^[5,6], as excellent field emitters (specifically $\text{W}_{18}\text{O}_{49}$)^[7] and as photo anodes in photochemical cells^[8]. In addition, WO_x have also found unique application in electrochromic devices due to their excellent voltage-modulated optical properties^[9]. Tungsten oxide (WO_3) is an n-type semiconductor with a reported band gap of about 2.6–2.8 eV^[10]. The intrinsic conductivity arises from its non-stoichiometric composition giving rise to a donor level formed by oxygen vacancy defect in the lattice. Since tungsten has many oxidation states, i.e., 2, 3, 4, 5 and 6, the tungsten compound can exist in many forms. For instance, the typical forms of tungsten oxides are tungsten(VI) oxide (WO_3 , lemon yellow appearance) and tungsten(IV) oxide (WO_2 , brown and blue appearance)^[11]. Such electronic properties make the tungsten oxides suitable for various applications such as electrochromic^[12], photochromic^[13], photocatalyst^[14], and gas sensors^[15–17]. Various methods including chemical vapour deposition^[18], electrochemical deposition^[19], laser vaporization^[20, 21] have been used to prepare tungsten oxide thin films. In conventional WO_3 thin films with nanoscale-sized grains, the electrical conduction is mainly controlled by free carrier transport across the grain boundaries. So the synthesis of mono crystalline tungsten oxide as nano wires or nanorods is of great interest. In the past years, Zhu et al.^[22] produced a micrometer scale tree-like structure by heating a tungsten foil, partly covered by SiO_2 in Ar atmosphere at 1600°C. These nanostructures were composed by monoclinic $\text{W}_{18}\text{O}_{49}$ nanoneedles and WO_3 nanoparticles. Nanorods of several oxides including WO_3 have been prepared by templating on acid-treated carbon nanotubes^[23]. By heating WS_2 in oxygen, fibers of $\text{W}_{18}\text{O}_{49}$ were produced with a pine-tree like structure^[24]. Mixtures of WO_2 and WO_3 with nanorods structure were obtained by Koltypin et al.^[25] via amorphous tungsten oxide nanoparticles. Li et al.^[26] have synthesized WO_3 nanobelts and nanorods via physical vapour deposition process where the nanostructures were deposited on silicon wafers maintained at 600°C. Recently Liu et al.^[27] reported on the preparation of tungsten oxide nanowires through a vapour-solid growth process by heating a tungsten wire partially wrapped with boron oxide at 1200°C and Shingaya et al.^[28] pre-

pared by oxidation at high temperature well-oriented WO_x nanorods on a (0. 01)W surface.

However, the study on nanoscaled WO_3 materials is still in its infancy due to lack of suitable preparation method. In the present work, we report a novel route for template synthesis of crystalline WO_3 nanorods. Our work on the tungsten oxide tubular structures featured a low cost and an easy manipulation technique. In the fabrication, no catalyst was involved and only a rough vacuum was required.

EXPERIMENTAL

Materials

All the chemicals used were of analytical grade. Phosphotungstic acid (Sisco Research Laboratories, India), dichloromethane and concentrated HF (Merck) were used. Alumina template membranes were obtained from Whatman Anopore Filters. Anodisc alumina membranes with a pore size of 200 nm and thickness of 60 μm were purchased from Whatman (catalog no. 6809-6022; Maidstone, U.K.).

Synthesis of Tungsten oxide nanorods.

10 g of Phosphotungstic acid ($\text{H}_3\text{PW}_{12}\text{O}_{40}$) was stirred in a 30 ml of methanol solution. The resulting colloidal suspension was infiltrated into the membrane under vacuum by wetting method. The same procedure was repeated 1 to 8 times. The upper surface of the membrane was then polished gently by sand paper (2500 grit) and dried at 368 K for 1 h. The formation of WO_3 nanorods inside alumina template (WO_3/AAO) was further achieved by programmed temperature thermal decomposition from 95 to 500°C min^{-1} and finally calcinated at 873 K for 3 h in air. The removal of the AAO template was performed by dissolving alumina template in 10% (v/v) HF. The WO_3 nanorod product was washed with a copious amount of deionized water, to remove the residual HF and dried at 393 K.

Characterization methods

The scanning electron micrographs were obtained after the removal of alumina template using a JEOL JSM-840 model, working at 15 keV. For transmission electron microscopic studies, the nanorods dispersed in ethanol were placed on the copper grid and the im-

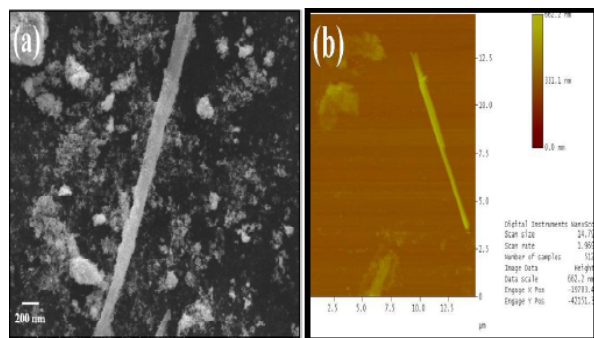


Figure 1 : (a) SEM Micrograph of the WO_3 nanorod and (b) AFM micrograph of the nanorod

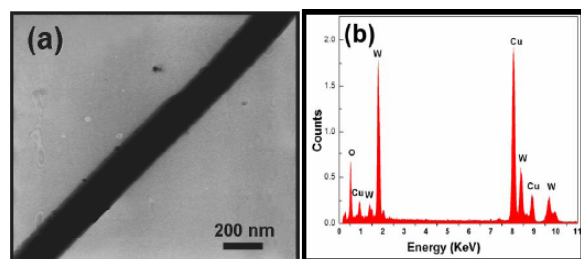


Figure 2 : (a) TEM Micrograph of the WO_3 nanorod and (b) EDS pattern of nanorod

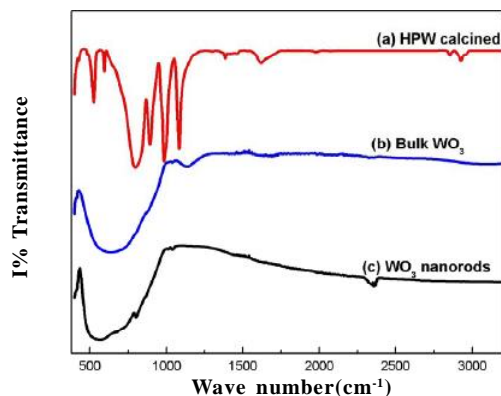


Figure 3 : FT-IR Spectrum of the (a) Calcined HPW (b) Bulk WO_3 and (c) WO_3 nanorods

ages were obtained using Phillips 420 model, operating at 120keV. The nanorods were sonicated in acetone for 20 minutes and then dropped on cleaned Si substrates. Next the AFM imaging was performed in air using a Nanoscope IIIA atomic force microscope (Digital Instruments, St. Barbara, CA) operated in contact mode.

The X-ray diffraction patterns were obtained on a Philips PW1820 diffractometer with CuK_α (1.54178 Å) radiation. The WO_3 nanorods placed in glass capillary tubes were used for recording Raman spectrum at room

temperature with 514.5nm excitation in backscattered mode using Bruker FRA106 FT-Raman instrument. The IR spectrum was recorded with Perkin-Elmer (L-710) spectrophotometer.

Electrochemical measurements

The catalyst was electrochemically characterized by cyclic voltammetry(CV) using an electrochemical analyzer(Bioanalytical Sciences, BAS 100). A common three-electrode electrochemical cell was used for the measurements. The counter and reference electrodes were a platinum plate(5cm^2) and a saturated Ag/AgCl electrode respectively. The CV experiments were performed using 1M H_2SO_4 solution at a scan rate of 50 mV/s. All the solutions were prepared by using ultra pure water (Millipore, $18\text{M}\Omega$). The electrolytes were degassed with nitrogen before carrying out the electrochemical measurements.

Preparation of working electrode

Glassy carbon (GC) (BAS Electrode, 0.07cm^2) was polished to a mirror finish with $0.05\mu\text{m}$ alumina suspensions before each experiment and this served as an underlying substrate of the working electrode. In order to prepare the composite electrode, the nanorods were dispersed ultrasonically in water at a concentration of 1mg ml^{-1} and $20\mu\text{l}$ aliquot was transferred on to a polished glassy carbon substrate. After the evaporation of water, the resulting thin catalyst film was covered with 5-wt% Nafion solution. Then the electrode was dried at 353 K and used as the working electrode.

RESULTS AND DISCUSSION

The morphology of tungsten oxide nanorods was studied with SEM, AFM, transmission electron microscopy (TEM) images on a Philips CM12/STEM instrument. The scanning electron microscopy (SEM) image presented in figure 1(a) shows the rod like morphology of the product. Further the AFM image confirms the rod like morphology in figure 1(b) which represents low magnification. The morphology of the nanorods can be confirmed with TEM micrograph shown in figure 2(a). The dimensions of the nanorods were matched with the outer diameter of the template used. The diameter of the nanorods was found to be around 200nm.

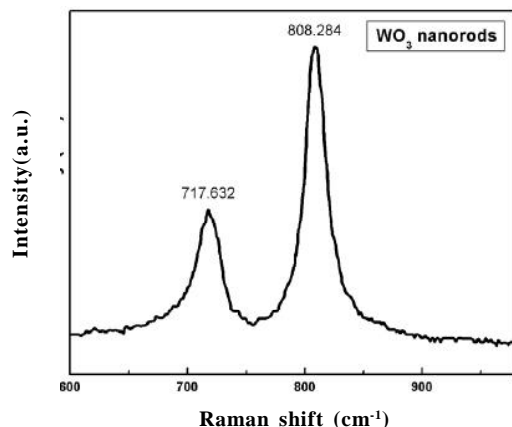


Figure 4 : Raman spectrum of the WO₃ nanorods

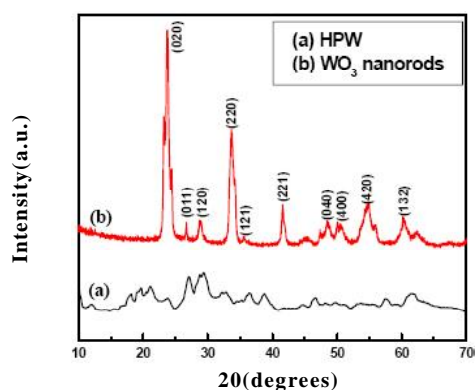


Figure 5 : XRD patterns of (a) HPW and (b) WO₃ nanorods

The composition of the nanorods was investigated using an energy dispersion spectroscopy (EDS). Figure 2(b) shows EDS of the WO₃ nanorods. EDS analysis indicates that the nanorods are mainly composed of W and O (the Cu signal comes from the TEM grids). No evidence of impurities was detected in the WO₃ nanorods.

The FT-IR spectra of WO₃ nanorods recorded in the region 400-3500cm⁻¹ are shown in figure 3. The broad band from 1000cm⁻¹ to 500cm⁻¹ corresponds to the W-O vibrational mode. It has been widely reported that HPW with Keggin structures gives several strong, typical IR bands at ca. 1079cm⁻¹(stretching frequency of P-O of the central PO₄ tetrahedron), 983cm⁻¹(terminal bands for W=O in the exterior WO₆ octahedron), 889 cm⁻¹ and 805 cm⁻¹(bands for the W-O_b-W and W-O_c-W bridge, respectively)^[29].

The raman spectra of WO₃ nanorods exhibiting bands at ~717 and 808cm⁻¹ are shown in figure 4. These bands agree closely to the wave numbers of the strongest modes of monoclinic-WO₃. The bands at 703 and

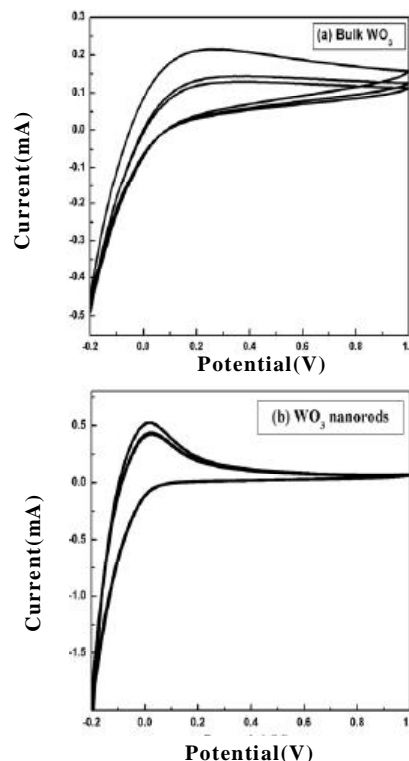


Figure 6 : Cyclic voltammograms for (a) Bulk WO₃ and (b) WO₃ nanorods in 1M H₂SO₄ at scan rate of 50mV s⁻¹ at 298K

813cm⁻¹ correspond to the stretching modes of the WO₃^[30-32]. The XRD pattern for the as-synthesized tungsten oxide nanorods and Phosphotungstic acid are given in figure 5(a,b) respectively. The diffraction peaks and the peak intensities of the tungsten oxide nanorods are in good agreement with the diffraction peaks of crystalline monoclinic phase of WO₃^[33,34].

The electrochemical behavior of bulk WO₃ and WO₃ nanorods were studied in 1M H₂SO₄ as shown in figure 6. The cyclic voltammogram shows an anodic peak current at -0.07V and it is due to the formation of tungsten bronzes by hydrogen intercalation in the tungsten trioxide. The electrochemical response due to W is seen at -0.1V in the forward scan, which matches with the peak reported in literature^[30]. Further, the stability of tungsten trioxides in sulphuric acid medium was evaluated by carrying out the cyclic voltammetry by repeating voltammetric cycles in 1M H₂SO₄. An initial decrease in current was observed and after few cycles the peak current remained the same even after 50 cycles and this confirms the stability of WO₃ nanorods in sulphuric acid medium.

CONCLUSIONS

In summary, a simple template synthesis method has been described for preparing WO₃ nanorods by a direct calcination of Phosphotungstic acid (HPW) in the channels of the alumina template. The size of nanorods is around 200nm which matches with the diameter of the template used. The Tungsten oxide nanorods with controlled morphology and composition have been achieved. The morphology of the aligned nanostructures was verified by SEM, AFM and TEM. It was found that WO₃ nanorods exhibit higher electrochemical activity and stability compared to bulk WO₃.

REFERENCES

- [1] P.Heszler, L.F.Reyes, A.Hoel, L.Landstrom, V. Lantto, C.G.Granqvist; Proc.Soc.Photo-Opt.Instrum. Eng., 5055, 106 (2003).
- [2] M.J.Madou, S.R.Morrison; Chemical Sensing with Solid State Devices, (1989).
- [3] G.Sberveglieri (Ed.); Gas Sensors, Kluwer, Dordrecht, The Netherlands, (1992).
- [4] Z.Liu, Y.Bando, C.Tang; Chem.Phys.Lett., **372**, 179 (2003).
- [5] M.Stankova, X.Vilanova, J.Calderer, E.Llobet, P.Ivanov, I.Gracia, C.Cane, X.Correig; Sens. Actuators, **B102**, 219 (2004).
- [6] J.L.Solis, S.Saukko, L.Kish, C.G.Granqvist, V. Lantto; Thin Solid Films, **391**, 255 (2001).
- [7] Y.Li, Y.Bando, D.Golberg; Adv.Mater., **15**, 1294 (2003).
- [8] C.Santato, M.Odzimkowski, M.Ulmann, J. Augustynski; J.Am.Chem.Soc., **123**, 10639 (2001).
- [9] C.G.Granqvist, E.Avendano, A.Azens; Thin Solid Films, **442**, 201 (2003).
- [10] M.A.Butler; J.Appl.Phys., **48**, 1914 (1977).
- [11] Solid state structure of tungsten trioxide. Available online at <http://www.webelements.com>.
- [12] C.G.Granqvist; Solar Ener.Mater., **60**, 201 (2000).
- [13] M.Sun, N.Xu, Y.W.Cao, J.N.Yao, E.G.Wang; J. Mater.Res., **15**, 927 (2000).
- [14] G.R.Bamwenda, H.Arakawa; Appl.Catal., **A210**, 181 (2001).
- [15] M.Akiyama, J.Tamaki, N.Miura, N.Yamazoe; Chem.Lett., **16**, 11 (1991).
- [16] A.A.Tomchenko, V.V.Khatko, I.Emelianov; Sens. Actuators, **B46**, 8 (1998).
- [17] D.S.Lee, S.D.Han, J.S.Hun, D.D.Lee; Sens. Actuators, **B60**, 57 (1999).
- [18] E.Brescacin, M.Basato, E.Tondello; Chem.Mater., **11**, 314 (1999).
- [19] Z.R.Yu, X.D.Jia, J.H.Du, J.Y.Zhang; Sol.Energy Mater.Sol.Cells, **64** 55 (2000).
- [20] M.Sun, N.Xu, J.W.Yao, E.C.Wang; J.Mater.Res., **15**, 927 (2000).
- [21] S.T.Li, M.S.El-Shall; Nanostruct.Mater., **12**, 215 (1999).
- [22] Y.Q.Zhu, W.Hu, W.K.Hsu, M.Terrones, N.Grobert, J.P.Hare, H.W.Kroto, D.R.M.Walton, H.Terrones; Chem.Phys.Lett., **309**, 327 (1999).
- [23] B.C.Satishkumar, A.Govindaraj, M.Nath, C.N.R. Rao; J.Mater.Chem., **10**, 2115 (2000).
- [24] W.B.Hu, Y.Q.Zhu, W.K.Hsu, B.H.Chang, M. Terrones, N.Grobert, H.Terrones, J.P.Hare, H.W. Kroto, D.R.M.Walton; Appl.Phys.A., **70**, 231 (2000).
- [25] Y.Koltypin, S.I.Nikitenko, A.Gedanken; J.Mater. Chem., **12**, 1107 (2002).
- [26] Y.B.Li, Y.Bando, D.Golberg, K.Kurashina; Chem. Phys.Lett., **367**, 214 (2003).
- [27] Z.Liu, Y.Bando, C.Tang; Chem.Phys.Lett., **372**, 179 (2003).
- [28] R.S.Wagner, W.C.Ellis; Trans.Met.Soc.AIME, **233**, 1053 (1965).
- [29] C.Santato, M.Odzimkowski, M.Ulmann, J. Augustynski; J.Am.Chem.Soc., **123**, 10639 (2005).
- [30] M.Figlarz; Prog.Solid-State Chem., **19**,1 (1989).
- [31] M.F.Daniel, B.Desbat, J.C.Lassegues, B.Gerand, M.Figlarz; J.Solid State Chem.**67**(2), 235 (1987).
- [32] S.H.Lee, H.M.Cheong, C.E.Tracy, A.Mascarenhaus, D.K.Benson, S.K.Deb; Electrochim.Acta **44**, 3111 (1999).
- [33] O.Yamaguchi, D.Tomihisa, H.Kawabata, K.Shimizu; J.Am.Ceram.Soc.**70**, 94 (1987).
- [34] P.M.Woodward, A.W.Sleight; J.Solid State Chem. **131**, 9 (1997).